Neurocomputing 564 (2024) 126969

Contents lists available at ScienceDirect

Neurocomputing

journal homepage: www.elsevier.com/locate/neucom

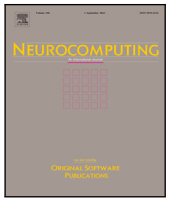

Analysis of synchronous localization systems for UAVs urban applications

Javier Díez-González *, Rubén Ferrero-Guillén, Paula Verde, Alberto Martínez-Gutiérrez, José-Manuel Alija-Pérez, Hilde Perez

Department of Mechanical, Computer and Aerospace Engineering, Universidad de León, León, Spain

ARTICLE INFO

Keywords:
UAV
Localization
TOA
TDOA
Cramér–Rao Bounds
Metaheuristics

ABSTRACT

Unmanned-Aerial-Vehicles (UAVs) represent an active research topic over multiple fields for performing inspection, delivery and surveillance applications among other operations. However, achieving the utmost efficiency requires drones to perform these tasks without the need of human intervention, which demands a robust and accurate localization system for achieving a safe and efficient autonomous navigation. Nevertheless, currently used satellite-based localization systems like GPS are insufficient for high-precision applications, especially in harsh scenarios like indoor and deep urban environments. In these contexts, Local Positioning Systems (LPS) have been widely proposed for satisfying the localization requirements of these vehicles. However, the performance of LPS is highly dependent on the actual localization architecture and the spatial disposition of the deployed sensor distribution. Therefore, before the deployment of an extensive localization network, an analysis regarding localization architecture and sensor distribution should be taken into consideration for the task at hand. Nonetheless, no actual study is proposed either for comparing localization architectures or for attaining a solution for the Node Location Problem (NLP), a problem of NP-Hard complexity. Therefore, in this paper, we propose a comparison among synchronous LPS for determining the most suited system for localizing UAVs over urban scenarios. We employ the Cràmer–Rao-Bound (CRB) for evaluating the performance of each localization system, based on the provided error characterization of each synchronous architecture. Furthermore, in order to attain the optimal sensor distribution for each architecture, a Black-Widow-Optimization (BWO) algorithm is devised for the NLP and the application at hand. The results obtained denote the effectiveness of the devised technique and recommend the implementation of Time Difference Of Arrival (TDOA) over Time of Arrival (TOA) systems, attaining up to 47% less localization uncertainty due to the unnecessary synchronization of the target clock with the architecture sensors in the TDOA architecture.

1. Introduction

Unmanned-Aerial-Vehicles (UAVs), usually referred to as drones, constitute a modality of vehicles whose use has grown significantly over the last few years. While initial design and development of UAVs were pursued for military applications, the innovation and the intended purposes of these devices has shifted into the civilian sector over the last decade [1].

The accessibility and the freedom of movement that these vehicles possess render them idoneous for a wide range of applications. Surveillance exercises [2], structural inspection [3], delivery services [4], industrial transport [5] and agricultural operations [6] represent actual research lines featured by these devices.

Furthermore, the interest in the insertion of UAVs into these fields resides in their capability for performing already existing tasks in a more efficient manner (e.g., transporting by air, easier access to high places). However, utmost efficiency is achieved when UAVs are capable of performing such tasks without the need for human intervention, thus carrying out these tasks autonomously.

Achieving autonomous behavior for UAVs represents a significant challenge and requires the cooperation of different subsystems within the aerial vehicle, which varies depending on the actual task to be conducted. Nevertheless, all UAVs applications rely on the adequate performance of a principal subsystem, the drone navigation and localization system.

Therefore, developing a robust, available and accurate localization system represents an essential step for implementing autonomous tasks in UAVs. Most commercial drones implement hardware for Global Navigation Satellite Systems (GNSS) localization (e.g., GPS, Galileo). While these localization systems offer global coverage, their localization

* Corresponding author.
E-mail address: jdieg@unileon.es (J. Díez-González).

https://doi.org/10.1016/j.neucom.2023.126969
Received 1 February 2023; Received in revised form 4 September 2023; Accepted 22 October 2023
Available online 29 October 2023

accuracy can result insufficient for certain applications or certain scenarios, such is the case of urban environments [7].

The Non-Line-Of-Sight (NLOS) and the multipath interference present in deep urban environments harshly penalize the reception of the satellite signal, while their interpretation usually results in significant localization uncertainties [8], which compromises the performance of activities such as delivery services in these scenarios [9].

In this context, localization systems based on Wireless Sensor Networks (WSNs) have been widely proposed throughout the literature for achieving improved localization accuracy over harsh and inconsistent scenarios [10]. Through the deployment of a set of low-cost sensors over a given scenario, WSNs constitute a wireless localization network with local coverage (i.e., Local Positioning Systems (LPS)). Contrary to satellite-based localization, LPS can adapt to any scenario by planning the spatial distribution of the beacons that constitute the localization network, which improves their accuracy and flexibility. Furthermore, unlike visual-based localization systems, which are quite common in the field of robotics, wireless LPS achieve higher reliability over variable weather and light conditions [11].

However, a wide variety of LPS are discussed throughout the literature that rely on different physical measurements for attaining the target location (e.g., power, angle, frequency) [12]. In this context, time-based localization systems represent one of the most extended technology due to their trade-off among accuracy, stability and accessibility [13].

These localization systems determine the UAV location through the measurement of different signal reception times. However, depending on how the beacons and the target interact, two different localization architectures are mainly proposed throughout the literature: Time of Arrival (TOA) [14] and Time Difference of Arrival (TDOA) [15].

Each architecture denotes different characteristics and follows different signal paths for achieving the target localization, which renders each localization architecture susceptible to different error sources (e.g., path loss, NLOS, clock errors). As a consequence of these differences, the performance of each architecture varies depending on the scenario of application.

Therefore, prior to deploying an extensive localization WSN, a comparative analysis among existing localization architectures should be taken into consideration for determining the most suited technology for each application and scenario characteristics.

In our previous works, we have performed comparisons between time-based localization architectures for different scenarios, yet particularized for low-elevation targets [16]. Nonetheless, to the author's best knowledge, there is no comparison available in the literature that focuses on studying the particularities of UAV localization in deep urban scenarios.

However, UAV localization over urban scenarios implies certain particularities in this problem. The higher elevation of UAV flight conditions reshapes the localization signal paths, which may result in variation in the predominance of each error source, thus varying the utmost achievable performance of a localization architecture.

Nevertheless, in order to achieve their maximum performance, LPS must deploy their sensors so that their coverage and localization accuracy are maximized. This optimization problem, defined as the Node Location Problem (NLP), entails an NP-Hard combinatorial complexity [17].

Different metaheuristic techniques have been proposed throughout the literature for attaining a near-optimal solution within a reasonable time, such as: genetic algorithms [18], differential evolution [19], or memetic algorithms [20]. These heuristic algorithms seek to optimize the Cramèr–Rao Bound (CRB), an unbiased estimator of the localization accuracy, a widely studied estimator in localization theory that serves as a performance evaluator for the localization system [21].

Therefore, in this paper, which extends the work of our previous conference [22], we implement for the first time to the author's best knowledge a node location optimization for UAV applications in urban scenarios for the two main time-based localization architectures (i.e., TOA and TDOA). In this context, we have devised a Black Widow Optimization (BWO) [23] for optimally deploying the beacons of the LPS. Furthermore, we characterize the noise, detecting the LOS and NLOS propagation conditions of the positioning signal through a ray-tracing algorithm, and the clock error sources for each localization architecture, consequently performing a comparison among time-based localization systems for the presented application.

Moreover, in order to improve the efficiency and performance of the attained sensor distribution, a Sensor Selection Problem (SSP) optimization is considered during the NLP optimization [24]. The SSP aims to determine the best combination of sensors for the localization of a target in space [25], which reduces the number of used sensors in use for each point while also reducing the localization uncertainties. Considering the SSP during the NLP optimization further increases the resulting accuracy of the network as stated in [26].

Therefore, the main contributions of this paper can be summarized through the following highlights:

- A novel analysis for optimally deploying time-based localization systems for UAV navigation in deep urban scenarios.
- The particularization of a BWO algorithm for attaining the NLP problem with different localization architectures.
- The proposal of a comparison among time-based localization architectures for UAVs in deep urban environments.

The remainder of this paper is organized as follows: Section 2 summarizes the related works of UAV localization and time-based localization architectures. In Section 3, a mathematical model is defined for performing the NLP and SSP combined optimization for the proposed application. Section 4 describes the CRB characterization for each proposed architecture while Section 5 details our devised BWO for the attained problem. Finally, Section 6 entails the results of this work and Section 7 presents the conclusions of this paper.

2. Related works

The deployment of UAVs in urban scenarios has been broadly discussed throughout the literature [27]. However, their implementation is still scarce due to regulatory statements [28] that can be successfully addressed for actual applications such as [29] and due to technical limitations such as their difficult integration in urban communications networks [30], energy constraints due to the limited use of their batteries [31], trajectory optimizations [32], or their localization in GNSS difficultly accessed areas [33].

Precisely, Mozaffari et al. [30] define that one of the main milestones to fully integrate drones in urban environments is the definition of localization systems that enable the precise navigation of UAVs.

In this sense, some proposals of the literature address this topic in different ways. For instance, Couturier and Akhloufi [34] review the absolute visual localization of UAVs through remote sensing image retrieval, the comparison of UAV images with satellites images registration, place recognition, or image geolocalization. Although these approaches attain remarkable results for the definition of the environment, these methods are dependent on visual images which supposes a considerable energy consumption that reduces the UAVs' autonomy.

Other authors such as Liu et al. [35] or Afifi et al. [36] proposed the deployment of a wireless network or the existing communications infrastructure respectively, for measuring the signal power decay of the localization signal emitted by the UAV to determine its localization. However, this approach is not suitable for dynamic environments such as dense urban scenarios in which the localization signal can be differently affected over time. This constitutes an unstable localization system non-suitable for the precision navigation of UAVs in urban environments.

Angle-based localization can also be considered to address the 3D localization of UAVs as proposed by Xu and Doğançay in [37]. This

work highlights the relevance of addressing an optimization of the location of the sensor nodes to achieve promising localization results. However, as for the previous power methods, angle-based localization is compromised in Non-Line-of-Sight (NLOS) and multipath typical urban dense environments.

Therefore, approaches based on time measurements are the most extended within the literature for providing stable, robust, and accurate navigation. However, different architectures achieve the localization of the target through different procedures. In this context, TOA system measures the total time-of-flight of the localization system from the UAV to the architecture nodes. On the other hand, TDOA systems employ the relative time-lapse measurements between the reception of the localization signal in two different architecture nodes [38].

In this sense, recent works highlight the benefits of employing both the TOA and the TDOA architectures for UAV applications in GNSS-denied environments. For instance, Lin and Zhan [39] fusion the TDOA system with visual procedures to enhance UAV navigation in indoor spaces or Liu et al. [40] explore the main error sources of the TOA architecture for UAV localization.

The differences between both approaches result in changes in the convenience of each architecture for each scenario of application. However, the performance of these architectures has not been compared in urban scenarios in a common framework to determine the suitability of each system for UAV localization.

In this manner, we extend in this work our previous conference paper [22] by analyzing not only the performance of the TDOA architecture for UAVs localization in urban environments but also analyzing the performance of one more synchronous architecture (i.e., TOA). This comparison is the first in the literature for these two localization methods for UAVs localization in urban scenarios.

Nevertheless, in order to perform a fair comparison, not only a common scenario for the deployment of each architecture must be considered but also an optimal location for the sensor nodes of each architecture. This is a consequence of the dependence of the localization results on the spatial location of the architecture sensor nodes.

Therefore, this optimization allows the definition of the best achievable performance for each architecture analyzed defining a fair framework for the comparison of the time-based architectures. Thus, we perform in this paper a sensor location optimization through the BWO metaheuristic introduced in [23] that enables the definition of optimal sensor networks for each architecture.

This optimization also entails a novelty in the UAVs localization field since none of the papers highlighted in this Section addresses the NLP optimization for reducing the localization uncertainties of each architecture. The mathematical model for the proposed optimization is presented in detail in Section 3.

3. Mathematical model

The performance of any LPS is heavily dependent on the distribution of the sensors that constitute the WSN over the studied region. The NLP aims to find the subset of optimal Cartesian coordinates (S_l) for each node of the localization system that maximizes the coverage region while minimizing the localization uncertainties, where (S_l) can be characterized as:

$$\langle S_l \rangle = \langle s_1, \dots, s_{n_s} \rangle; \quad s_i = (x_i, y_i, z_i); \quad i \in \{1, \dots, n_s\} \tag{1}$$

where s_i represents the Cartesian coordinates of sensor i and n_s is the total number of sensors deployed. In this sense, the subset that entails the optimal sensor distribution (S_l) is contained within the set of all possible sensor distributions (S). The dimension of set (S) can be deduced from the combinatorial nature of the NLP, resulting in the following expression [41]:

$$C = \prod_{i=1}^{n_s} (n_{NLE} - i) \tag{2}$$

where C is the number of possible solutions and n_{NLE} is the total number of discretized points for representing the Node Location Environment (NLE) during the optimization, thus representing the total number of possible sensor locations.

Nevertheless, this optimization must consider different restrictions regarding the valid locations of sensors in space and the architecture requirements of coverage and minimum number of sensors to assess the target location. These restrictions can be described for each localization architecture under the following mathematical model of the NLP:

$$\text{Maximize}: \; Z = ff(ff_{CRB}, ff_{pen}) \tag{3}$$

Subject to:

$$\begin{gathered} x_{lim_1} \le x_i \le x_{lim_2} \; \forall x_i \in s_i; \; s_i \in S; \; s_i \notin U \\ y_{lim_1} \le y_i \le y_{lim_2} \; \forall y_i \in s_i; \; s_i \in S; \; s_i \notin U \\ z_{lim_1} \le z_i \le z_{lim_2} \; \forall z_i \in s_i; \; s_i \in S; \; s_i \notin U \\ cov_k \ge n_{min} \; \forall k \in \{1, \dots, n_{TLE}\} \end{gathered} \tag{4}$$

$$\begin{gathered} cov_k = \sum_{i=1}^{n_s} cov_{ki} \cdot \zeta_i \\ cov_{ki_{TOA|TDOA}} = \begin{cases} 1 & \text{if} \quad SNR_{ki} \ge SNR_{threshold} \\ 0 & \text{if} \quad \text{otherwise} \end{cases} \end{gathered} \tag{5}$$

where ff_{CRB} and ff_{pen} are fitness functions based on the Cramèr–Rao error characterization and the devised penalizations for not attaining the restrictions of the optimization; $x_{lim_1}, y_{lim_1}, z_{lim_1}$ and $x_{lim_2}, y_{lim_2}, z_{lim_2}$ represent the lower and upper limits of the scenario discretization; U is the subset containing all forbidden regions for the location of the sensors in the environment; cov_k represents the number of sensors under coverage for point k of the Target Location Environment (TLE) (i.e., each possible target location); n_{min} is the minimum number of sensors under coverage required for each architecture to achieve the target location (i.e., three and four for the TOA and the TDOA architectures respectively as demonstrated in [42]); n_{TLE} is the number of discretized points for the TLE; cov_{ki} is a step function of value 1 when point k is within coverage of sensor i and 0 otherwise; SNR_{ki} represents the signal-to-noise ratio, measured between the TLE point k and sensor i, and $SNR_{threshold}$ defines the SNR that determines a signal link among effective coverage.

Furthermore, in our proposal, we attain the NLP and the SSP simultaneously through the consideration of the SSP within the performance analysis of each sensor distribution from the NLP. This combined analysis guides the optimization into reaching a more adequate solution than a bare NLP approach, as proven in our past works [43].

In this context, the SSP aims to obtain the set of the sensors under coverage within a certain TLE point k, $(S_l'(k))$, which is contained within the set that entails all sensors under coverage of k, $(S_l(k))$. As a consequence, not all sensors within coverage of point k are utilized for its localization, ζ_i is a boolean variable that values 1 when sensor i is considered for performing localization in point k, and 0 otherwise.

Nevertheless, the proposed optimization model that entails the NLP and SSP is based upon the definition of the CRB for evaluating the performance of a given sensor distribution. The different characterization model, which we will disclose in the following Section, result in the obtention of a localization uncertainty for each TLE point, measured from the Root Mean Squared Error (RMSE) of trace of the inverse of the Fisher Information Matrix (FIM).

From this CRB characterization, the SSP evaluates which combination of sensors achieves the best performance, thus selecting the optimal combination of sensors for each point. Therefore, we can define the previously discussed fitness functions through the following equations:

$$ff = c_1 \cdot ff_{CRB} - c_2 \cdot ff_{pen} \tag{6}$$

$$ff_{CRB} = \frac{1}{n_{TLE}} \sum_{k=1}^{n_{TLE}} \left(1 - \frac{RMSE(S'(k))}{RMSE_{ref}}\right) \tag{7}$$

$$ff_{pen} = \frac{1}{n_s} \sum_{i=1}^{n_s} R_i; \quad R_i = \begin{cases} 1 & \text{if} \quad s_i \in U \\ 0 & \text{if} \quad \text{otherwise} \end{cases} \tag{8}$$

where c_1 and c_2 are parameters adjusted for weighting each fitness function importance in the optimization; $RMSE_{ref}$ represents the accuracy reference $RMSE$, equivalent to the maximum valid achievable $RMSE$ value in the analyzed scenario obtained experimentally [20,44], thus constricting the ff_{CRB} domain in the interval $[0, 1]$ and R_i is a boolean variable that indicates if a given sensor i is located within the admissible regions.

Furthermore, evaluating of the fitness function with the best combination of sensors for each point attains a superior performance of the localization network, given a fixed distribution of sensors. However, the consideration of this analysis during the optimization guides the resulting solutions of the optimization into a sensor network with better accuracy when SSP is applied with respect of a traditional NLP optimization, which would only underwent the SSP in its final solution [26].

Therefore, the consideration of both problems simultaneously further improves the performance of the optimized localization network when applying sensor selection, thus serving as an interesting guideline for the proposed comparison of this paper.

However, implementing the proposed mathematical model for each localization architecture requires the definition and particularization of the CRB for each studied architecture, an analysis that we attain in the following Section.

4. Cramér-Rao Bound

Localization systems are affected by the degradation of the positioning signal during its signal path [45], also sustaining uncertainties due to imperfect measurements of the physical property used to determine the target location (i.e., time measurements in this paper) [46].

This promotes that the algorithms in charge of calculating the target location cannot guarantee the attainment of the actual location of the target. In fact, the best localization algorithms are those that minimize the accumulated uncertainties in the set of measurements in order to provide the most reduced error in the position calculation [47].

In this sense, the lower bound for the localization error can be obtained from the Cramér–Rao Lower Bound (CRLB). The CRB allows the obtainment of the lower variance of an unbiased estimator of a deterministic unknown parameter [48] (i.e., the spatial coordinates of the target in the localization field).

In this context, the CRB allows the definition of the minimum achievable error by any localization algorithm used for determining the target location [49]. This constitutes the CRB as an indicator of the maximal performance of a localization system regardless of the localization algorithm implemented to calculate the target location [50].

However, when considering some stochastic parameters such as the clock error characterization of this paper, the CRLB does not indicate a real achievable bound since positive or negative deviations of the parameter would either reduce or increase the error bound accidentally. In these cases with stochastic conditions, it is more accurate to obtain the expected values of error by performing a Monte-Carlo simulation as we address in this paper, thus defining a novel more representative error bound defined as the Cramér–Rao Bound (CRB).

Consequently, under these conditions, the CRB is widely proposed for comparing the capabilities of different localization sensor deployments and recently has been used as the fitness indicator of the NLP metaheuristic optimizations. Based on the evaluation of the CRB, these optimizations are capable to reach optimal sensor arrangements that minimize the localization error [18,51,52], and maximize the coverage region of the system [53], following the mathematical model presented in Section 3.

Therefore, in this Section, we present a generic model for defining the Fisher Information Matrix (i.e., the inverse of the CRB) as well as the method to measure the localization accuracy based on such model in Section 4.1. The generic model is then particularized for the TOA and TDOA time-based architectures considered in this paper in Sections 4.2 and 4.3 respectively.

4.1. CRB matrix form definition for localization architectures

The FIM, from which the CRB is attained, can be expressed through the following matrix form [50]:

$$FIM_{mn} = \left(\frac{\delta h(TS)}{\delta TS_m}\right)^T \boldsymbol{R}^{-1}(\boldsymbol{TS}) \left(\frac{\delta h(TS)}{\delta TS_n}\right) + \frac{1}{2} tr\left\{\boldsymbol{R}^{-1}(\boldsymbol{TS}) \left(\frac{\delta R(TS)}{\delta TS_m}\right) \boldsymbol{R}^{-1}(\boldsymbol{TS}) \left(\frac{\delta R(TS)}{\delta TS_n}\right)\right\} \tag{9}$$

where FIM_{mn} represents the FIM element calculated considering the Target Sensor (TS) coordinates m and n; $\boldsymbol{h}(TS)$ is the vector containing the information of the signal path of each architecture, and $\boldsymbol{R}(TS)$ is the covariance matrix of the architecture at study.

This allows a flexible characterization of the error uncertainties of the localization system through a complete definition of the covariance matrix of each architecture and through the definition of the signal path followed by each localization system.

In this paper, we characterize the system uncertainties considering the two main error sources that affect localization time-based systems in outdoor urban environments (i.e., noise in LOS/NLOS conditions and clock errors).

These two errors can be considered independently since the degradation of the localization signal during its path from emitter to receiver and the uncertainties generated during the measurement of the time-of-flight of the positioning signal are separate factors, yet both influential on the localization errors [26].

Therefore, when building the covariance matrix ($\boldsymbol{R}$) of each architecture, noise and clock uncertainties can be combined as follows:

$$\sigma^2_{architecture_{ij}} = \sigma^2_{architecture(noise)_{ij}} + \sigma^2_{architecture(clock)_{ij}} \tag{10}$$

where $\sigma^2_{architecture}$ represents the total variance/covariance of the element R_{ij}; $\sigma^2_{architecture(noise)_{ij}}$ is the variance/covariance related to noise uncertainties, and $\sigma^2_{architecture(clock)_{ij}}$ is the variance/covariance related to clock uncertainties.

Once built the covariance matrix, $\boldsymbol{R}(TS)$, and the signal spatial propagation vector, $\boldsymbol{h}(TS)$, the FIM can be directly determined through Eq. (9).

This allows, as stated in [54,55], the definition of the Root Mean Squared Error (RMSE) in a particular TS location through the inverse of the FIM (i.e., the CRB):

$$RMSE_{UAV_k} = \sqrt{trace(\mathbf{FIM^{-1}})} \tag{11}$$

where $RMSE_{UAV_k}$ is the lower RMSE achievable in a particular location k considered for the UAV navigation in the coverage area of the deployed localization architecture.

As shown in this subsection, this generic and flexible error characterization can be adapted to the particularities of each localization architecture analyzed through the definition of the signal path $\boldsymbol{h}(TS)$ and the covariance matrix $\boldsymbol{R}(TS)$.

For this purpose, as presented in the next subsections, we characterize the noise uncertainties following a heteroscedastic model, as required for LPS applications [56]. This characterization includes the noise uncertainties in LOS environments, modeled through a Log-Normal path loss model as in [57], which is enriched by the differentiation of the LOS/NLOS paths defined through a ray tracing algorithm as introduced in [58].

In addition, the clock error uncertainties of each architecture include the definition of the errors produced due to the clock drift and initial-time offset as proposed in [46] to which we added the truncation error of the instrumentation [43].

This combination of noise and clock errors represents the most complete error characterization in urban environments in the literature to the authors' knowledge. In the next subsections, the definition of each error is defined for the two architectures analyzed in this paper (i.e., TOA and TDOA).

4.2. TOA error characterization

TOA architecture measures the total time-of-flight of the positioning signal from an emitter to a receiver. It is a synchronous architecture that requires the synchronization of the TS clock with all the architecture sensors' clocks, defining a common framework to determine every time measurement involved in the positioning calculation [59].

Therefore, the $\boldsymbol{h}$ vector of the TOA architecture can be defined as follows:

$$h_{TOA_i} = \left\| TS - CS_i \right\|; \quad i = 1, \dots, n_{CS} \tag{12}$$

where n_{CS} is the total number of coordinator sensors of the TOA architecture under effective coverage considered for the positioning calculation in the point of study after addressing the SSP as introduced in Section 3.

As for the covariance matrix of the TOA system, since the time measurements are uncorrelated [60], the non-diagonal elements of the matrix are equal to zero. For the diagonal terms, we present hereafter the characterization of the noise and clock uncertainties.

The noise uncertainties are characterized through the Log-Normal path loss model resulting in the following expression:

$$\sigma^2_{TOA(noise)_{ii}} = \frac{c^2}{B^2(\frac{P_T}{P_N})} PL(d_0) \left[\left(\frac{d_{i_{LOS}}}{d_0} \right)_{CSi} + \left(\frac{d_{i_{NLOS}}}{d_0} \right)^{\frac{n_{NLOS}}{n_{LOS}}}_{CSi} \right]^{n_{LOS}} \tag{13}$$

$$d_{i_{LOS}} = \left\| TS - CS_i \right\|_{LOS} \tag{14}$$

$$d_{i_{NLOS}} = \left\| TS - CS_i \right\|_{NLOS} \tag{15}$$

where c is the speed of the radioelectric waves; B the signal bandwidth; P_T the transmission power of the localization signal; P_N the mean noise power calculated through the Johnson-Nyquist equation; $PL(d_0)$ the path loss at the reference distance d_0 for which we consider 10 m in this paper as stated in [61] for urban propagations; $d_{i_{LOS}}$ and $d_{i_{NLOS}}$ are the LOS/NLOS distances covered by the positioning signal from the TS to the CS i respectively, and n_{LOS} and n_{NLOS} are the path loss exponents in LOS/NLOS environments respectively.

In addition to the noise characterization, the clock uncertainties produced as a consequence of imperfect time measurements are modeled as follows:

$$\sigma^2_{TOA(clock)_{ii}} = \frac{1}{n_{MC}} \sum_{k=1}^{n_{MC}} \left\{ \left| T_i - floor_{TR} \left[(T_i + U_i - U_0 + T_0(\eta_i - \eta_0) + T_i\eta_i) \right] \right| c^2 \right\} \tag{16}$$

where n_{MC} are the number of Monte Carlo simulations performed to estimate the expected value of the clock variance following the model introduced in [43]; T_i is the ideal time-of-flight of the positioning signal from the TS to a particular CS_i; $floor_{TR}$ refers to the truncation of the time measurement due to the physical characteristics of the clock; U_i and U_0 are the ideal time lapses from the last synchronization of the CS_i and TS clocks respectively; T_0 is the interval between the end of the last synchronization process and the emission of the positioning signal and η_i and η_0 are the clock drifts of the CS_i and the TS respectively.

4.3. TDOA error characterization

TDOA architecture is based on the measurement of the different arrival times of the positioning signal to two distinct architecture receivers [62].

By only measuring the time difference of arrival, the TDOA architecture achieves independence from the timestamp of the signal emission. As a consequence, the synchronization of the TS clock with the architecture sensors clocks is unrequired, although the synchronism among the architecture sensors is still mandatory.

This builds a localization process consisting of two different signal paths, as considered in the $\boldsymbol{h}$ vector of the TDOA architecture:

$$h_{TDOA_m} = \left\| TS - CS_i \right\| - \left\| TS - CS_j \right\| \quad i = 1, \dots, n_{CS}; \quad j = 1, \dots, n_{CS}; \quad i \neq j \quad m = 1, \dots, n_{CS} - 1 \tag{17}$$

where i and j represent the two positioning signal paths involved in the TDOA measurement and m refers to the time measurement considered for the positioning calculation.

Although two different paths are considered, their measurements are correlated as introduced in [60]. Thus, the non-diagonal terms of the covariance matrix are distinct from zero in the TDOA architecture. From this base, noise and clock uncertainties are built into the TDOA error model of this paper.

Noise characterization follows the same model as in the TOA architecture but considering the two signal paths:

$$\sigma^2_{TDOA(noise)_{ij}} = \frac{c^2}{B^2(\frac{P_T}{P_N})} PL(d_0)\ \kappa_{ij} \tag{18}$$

$$\kappa_{ij} = \left[\left(\frac{d_{i_{LOS}}}{d_0} \right)_{CSi} + \left(\frac{d_{i_{NLOS}}}{d_0} \right)^{\frac{n_{NLOS}}{n_{LOS}}}_{CSi} + \left(\frac{d_{j_{LOS}}}{d_0} \right)_{CSj} + \left(\frac{d_{j_{NLOS}}}{d_0} \right)^{\frac{n_{NLOS}}{n_{LOS}}}_{CSj} \right]^{n_{LOS}} \tag{19}$$

$$d_{j_{LOS}} = \left\| TS - CS_j \right\|_{LOS} \tag{20}$$

$$d_{j_{NLOS}} = \left\| TS - CS_j \right\|_{NLOS} \tag{21}$$

where $d_{j_{LOS}}$ and $d_{j_{NLOS}}$ refer to the LOS/NLOS distance traveled by the positioning signal to the CS_j and determined through the ray tracing algorithm introduced in [58].

Clock uncertainties characterization considers both time measurements required to define an equation of potential target locations:

$$\begin{aligned} \sigma^2_{TDOA(clock)_{ij}} = & \frac{1}{n_{MC}} \sum_{k=1}^{n_{MC}} \left\{ \left| T_i - floor_{TR} \left[(T_i + U_i - U_0 + T_0(\eta_i - \eta_0) + T_i\eta_i) \right] \right| c^2 \right\} \\ & + \frac{1}{n_{MC}} \sum_{k=1}^{n_{MC}} \left\{ \left| T_j - floor_{TR} \left[(T_j + U_j - U_0 + T_0(\eta_j - \eta_0) + T_j\eta_j) \right] \right| c^2 \right\} \end{aligned} \tag{22}$$

where T_j represents the ideal time-of-flight of the positioning signal from the TS to the CS_j; U_j is the ideal time-lapse from the last synchronization of the CS_j clock and η_j is the drift of the CS_j.

All these characterizations of the $\boldsymbol{h}$ vector and the covariance matrix $\boldsymbol{R}$ of each architecture allow building the FIM matrix of Eq. (9) which is later used in Eq. (11) to calculate the RMSE associated with a particular location covered by the architecture at study.

As introduced in Section 3, this error is calculated in each point under coverage (i.e. in this paper the area for UAVs navigation) in order to build a robust, accurate, and stable localization model for the UAVs. As introduced previously, this requires an optimization of the

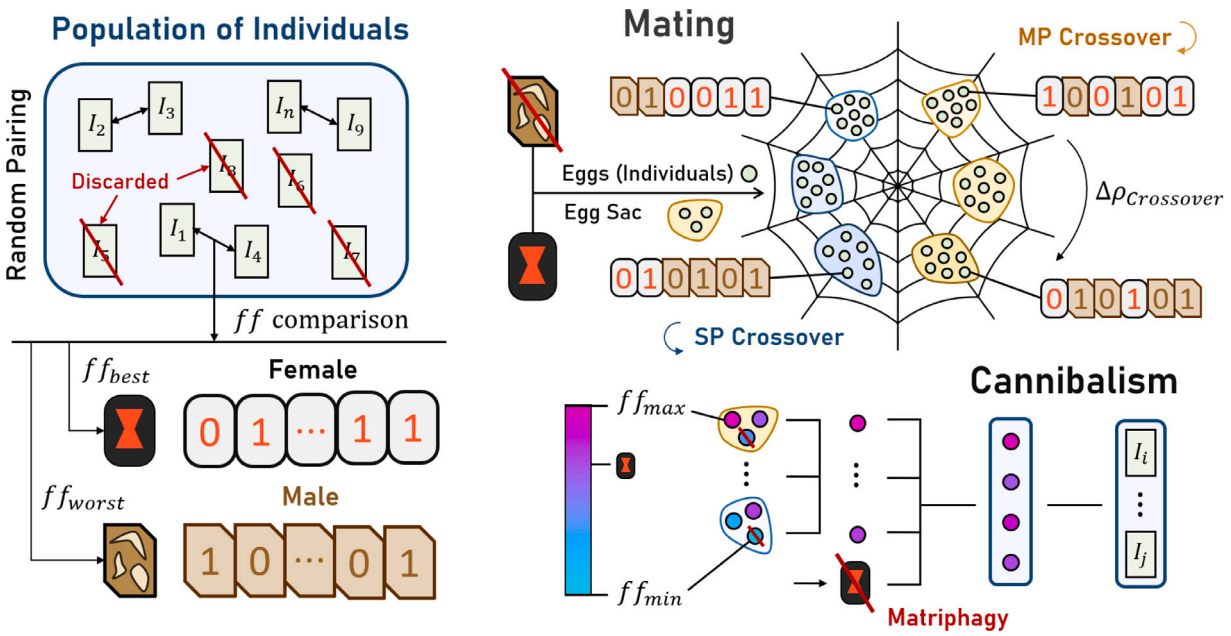

Fig. 1. Representation of the BWO unique operators of mating and cannibalism.

sensors' location of each architecture in order to achieve an optimal performance of the localization system. In this paper, we propose to address this optimization through the BWO metaheuristic that we present in Section 5.

5. Black Widow optimization for localizing the architecture nodes of time-based positioning systems

Black Widow optimization was proposed by Hayyolalam and Kazem in 2020 [63]. It is based on the unique mating of black widows in which the male dies after reproduction. This particular reproduction of black widows inspired the previous authors to build a novel metaheuristic with strong diversification properties to explore difficulty-accessed spaces of solutions in complex mathematical combinatorial problems.

We proposed in [23] the adaptation of the BWO for the NLP in localization systems. Results showed an improvement of previous approaches [64] demonstrating the benefits of this optimization technique to address discontinuous fitness landscapes such as the optimization considered in this paper.

The discontinuity of the fitness function in the localization NLP is a consequence of the LOS/NLOS links of the positioning signal with the sensors of the architecture [20]. A steep jump in the fitness values is made depending on whether or not an NLOS-type connection is produced during the transmission of the localization signal to the architecture nodes. Therefore, the BWO is a suitable candidate to optimize the location of the sensors of the two architectures analyzed in this paper (i.e., TOA and TDOA) in order to perform a fair comparison of the capabilities of each architecture for UAVs localization in urban environments.

BWO fundamentals are built under population-based metaheuristic principles. As a consequence, a number of candidate solutions to the NLP (i.e., the population) are subjected to an evolutionary process to achieve optimized solutions [65]. This implies applying genetic operators to adapt the individuals (i.e., each potential solution considered in the population) to an environment dominated by the NLP conditions introduced in Section 3.

The differences between the BWO and traditional population-based metaheuristics such as genetic algorithms [65] or differential evolution [66] lies in the modification of the genetic operators based on the reproduction of black widows.

In the BWO, the mating between the population individuals implies the father's death (i.e., the less adapted individual of the two involved during the mating process). In addition, mating supposes the generation of numerous offspring (i.e., eggs), organized in clusters (i.e., egg sacs), where each egg is composed of the parents genotype. At this point, a novel and unique operator of the BWO process takes place, the cannibalism operator.

Cannibalism supposes the competition of the offspring inside each egg sac to guarantee the survival of only the best-adapted offspring in order to concentrate the mother's resources only on the most promising offspring. Cannibalism is produced through the comparison of the fitness values of the offspring.

However, cannibalism is also extended in the last stage of the process to the mother, since the mother can also be eaten by her offspring in case they are better adapted to the NLP than their mother (i.e., matriphagy).

We present in Fig. 1, the adaptation of this process to the NLP in which we perform a binary codification of the individuals of the population as presented in [18] and we use different crossing procedures (i.e., single point (SP) and multipoint (MP) crossovers), and different crossover percentages ($\rho_{Crossover}$) for the different egg sacs, as introduced in [23].

Later on, the remaining genetic operators of the population-based metaheuristics (i.e., mutation, selection, and elitism) are applied to generate and select the final individuals of the next generation unless the stopping criteria of the optimization have been reached (i.e., the number of generations fixed for the optimization or final convergence of the individuals of the population).

In this way, further analysis of the space of solutions is attained, allowing for obtaining optimized node deployments for each architecture analyzed.

In the next subsection, we present a pseudo-code of the BWO addressed considering the mathematical model presented in Section 3 for which the fitness function is built upon the CRB defined in Section 4.

5.1. Pseudo-code of the proposed BWO

Implementing the BWO requires particularizing all the methodology characteristics of the problem at hand. In this context, each individual within the algorithm should represent a valid solution for the NLP

(i.e., a specific sensor distribution). In our proposal, the individuals carry multiple binary chains, where each chain translates to a single node location in space, following the binary escalation procedure introduced in [18].

Through the previously described codification, the proposed BWO implements different genetic operators for guiding the optimization convergence into an optimized solution. Algorithm 1 represents the structure of the devised BWO with its particularization for the NLP.

Algorithm 1: BWO for the NLP (*N, Scenario*)

$\pi, OA, TLE, NLE \leftarrow$ Import Scenario;
Population $\leftarrow$ Initialization of N individuals within the NLE boundaries;
while $(Iteration \leq N_{gen})$ ***or*** $(Similarity < S_{max})$ **do**
  for *Individual* ***in*** *Population* **do**
    $ff_{CRB} \leftarrow$ Calculation of the lowest localization uncertainty of the TLE with sensor selection (*Individual*, π, n_{TLE}, *Architecture*, $SNR_{threshold}$);
    $ff_{pen} \leftarrow$ Fitness Penalization for node placing within prohibited regions ($Individual$, OA);
    $ff \leftarrow$ Fitness function evaluation (ff_{CRB}, ff_{pen});
  end
  Elitists $\leftarrow$ Selection of the Elitists (*Population*);
  Population $\leftarrow$ BWO Mating and Cannibalism (*Population*);
  Population $\leftarrow$ Mutation (*Population*);
end
Final Solution $\leftarrow$ Most fitted individual;
Output: *Final Solution*;

The devised algorithm commences by importing the scenario of simulation and all associated parameters (e.g., TLE and NLE region). Once imported, the BWO starts by initializing the population of individuals through the proposed codification.

The BWO then executes multiple iterations over the generated population, evaluating the performance of each individual (i.e., a specific sensor distribution) and implementing different genetic operators so that the population may converge to the optimal solution.

The fitness evaluation, which quantifies the degree of adaptation of each individual, is based on the previously discussed CRB, thus depending on the architecture at hand. It is within this fitness adaptation where the SSP is included along the NLP optimization, evaluating the individuals based on their performance over the NLP and SSP considerations.

More specifics on how Eqs. (9)–(22) are evaluated in the fitness functions are available in our previous work [26]. Moreover, the achieved performance of each individual is then compensated with the plausible penalizations generated by incorrect placements, thus constituting the overall fitness value.

Based on the achieved fitness value, the best fitted individuals are preserved through generations by means of the elitism operator. This operator safeguards the most adapted individuals, introducing intensification in the convergence to the final solution. The resulting population delivered by this operator is then exposed to the mating and cannibalism operators, the specific genetic operators of the BWO.

Algorithm 2 details the different steps that the algorithm undergoes in order to generate the following offspring (i.e., the next generation of individuals). In our proposal, we perform a Tournament 2 selection of the parents for discarding a certain number of individuals. The remaining parents are them randomly grouped in pairs for the mating, where the female and male roles are assigned to each parent depending on its fitness value.

For each pair of parents, multiple eggs sacs containing numerous offspring (i.e., eggs) are generated following different crossover procedures with different number of parents alleles percentages.

The elevated number of individuals achieves a higher exploration of the space of solutions, which combined with the intensification

Algorithm 2: BWO Mating and Crossover Operators (*Population*, *L*, *M*, $\Delta\rho_{crossover}$)

Selected Individuals, *Discarded Individuals* $\leftarrow$ Tournament 2 selection (*Population*);
Parents $\leftarrow$ Random Pairing (*Selected Individuals*);
for ***each*** *Pair* ***of*** *Parents* **do**
  Female Black Widow $\leftarrow \underset{parent \in Pair}{\text{argmax}}\ ff(parent)$;
  Egg Sacs $\leftarrow$ Mass Offspring generation with MP2 and SP crossover ($\Delta\rho_{crossover}$);
  $ff_{eggs} \leftarrow$ Fitness evaluation of each egg (*Egg Sacs*);
  Best Eggs $\leftarrow$ **For** ***each*** *Egg Sac* **in** *Egg Sacs*, Best *L Eggs* with highest ff_{egg} ***in*** *Egg Sac*;
  New Population (*Pair*) $\leftarrow$ Best *M Individuals* with highest ff **in** [*Best Eggs*, *Female Black Widow*];
end
Output: *New Population*;

introduced by the subsequent cannibalism operator guides the optimization convergence into the optimal solution.

The cited cannibalism operator takes place once all egg sacs have been generated. Within this genetic operator, the eggs inside each egg sac compete within each other based on their fitness value, which drastically reduces the number of remaining offspring.

Following the first round of egg selection, the cannibalism operator performs a second comparison between the remaining eggs from the egg sacs and the initial female black widow. This second round results in an additional severe reduction of the generated offspring, where only the most fitted individuals persist. The introduction of the female black widow into this phase supposes an additional intensification mechanism, granting the prevalence of the originated parent if a higher fitness value exists.

The resulting individuals from the mating of each parent pairs constitutes the next generation of the BWO population, which undergoes a mutation operator back in Algorithm 1. The resultant population are then reevaluated, repeating the described loop until the convergence criteria is met (i.e., maximum number of generations or similarity percentage among individuals).

The equilibrium between exploration and intensification capabilities denoted by this algorithm represents a robust methodology for attaining a near-optimal solution for all the optimizations required for the proposed comparison of this work.

In the following Section, we present the characteristics of the devised scenario and all the influential simulation hyperparameters, followed by a representation and a discussion of the achieved results.

6. Results

6.1. Scenario

In order to perform a valid comparison among localization architectures, a common framework needs to be proposed for evaluating and fairly contrasting the performance of each architecture.

Therefore, a common scenario of experimentation is proposed for the following analysis. The devised scenario, shown in Fig. 2, depicts a deep urban environment with buildings of different dimensions. These buildings represent obstacles for the deployment of sensors, thus constituting the Obstacle Area (OA) of our scenario [64]. Around these buildings, multiple roads traverse the scenario, thus representing a common urban environment with a high density of obstacles.

As indicated in Fig. 2, an airway for UAV transit has been situated above the different roads, which constitutes the TLE of our sensor distribution optimization. On the other hand, the sensors of the localization systems can be positioned over the building's roof and above the streets,

Table 1
Dimensions and characteristics of the proposed scenario configured for the optimization.

Parameter	Value
Area	23 000 m^2
Scenario dimensions	$x \in [0, 143]$ m $y \in [0, 161]$ m
Building height	$z_{obs} \in [29, 37]$ m
Airway height	$z_{UAV} \in [16, 20]$ m
Number of TLE points	28 701 points
Number of NLE points	4 194 304 points
TLE discretization	$\Delta x \equiv \Delta y \equiv 1$ m; $\Delta z = 0.5$ m
NLE discretization	$\Delta x = 0.63$ m $\Delta y = 0.56$ m $\Delta z = 0.1$ m

Table 2
Parameters of configuration for the channel of communications for the LPS architectures [67].

Parameter	Value
Transmission power	1 W
Frequency of emission	5465 MHz
Bandwidth	100 MHz
Mean noise power	−94 dBm
Receptor sensibility	−90 dBm
LOS exponent	2.1
NLOS exponent	4.1

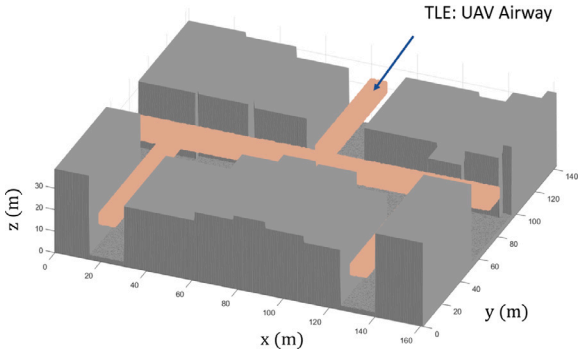

Fig. 2. Deep urban scenario for the proposed comparison among time-based localization architectures.

leaving a certain margin for not interfering with the traffic, which constitutes the NLE of our study.

Moreover, Table 1 specifies the particularities of the proposed scenario for the proposed comparison. The discretization stated for the TLE and the NLE pretends to represent a continuous region for both location environments.

6.2. Hyperparameters

Section 4 detailed the generation of a CRB model that allows the estimation of the UAV locations considering the path loss errors (i.e., noise and LOS/NLOS conditions) and clocks errors. Scenario conditions and channel characteristics influence the error caused by signal attenuation during communication between the transmitter and the receiver. Hence, the minimization of this error, especially in the vertical coordinate, reduces the uncertainties introduced in the target location measurement.

Table 2 specifies the configuration of the network technology and the environment properties (e.g., path loss exponents) that affect the signal and are used to perform the simulations.

In addition, the LPS based on time measurements suffer the uncertainties associated with the existence of temporal instabilities in the measurement clocks, which are modeled as a function of the initial offset and clock drift.

Table 3
Configuration parameters for the clocks of the TOA and TDOA architectures [46].

Parameter	Value
Time-Frequency product	1
Clock frequency	1 GHz
Frecuency-drift	U{−10,10} ppm
Initial-time offset	U{15,30} ns

Table 4
Values used by the BWO, for the optimization of the sensor arrangements of the TOA and TDOA architectures [22,68].

Parameter	Value
Population	80
Stop criteria	100 generations or convergence
Selection operator	Tournament 2
Crossover operator	Single and multipoint
Mutation operator	2%
Elitism operator	7%
Female BW alleles	20%/40%/60%/80%
Procreation rate	24
Cannibalism rate	85%
Survival rate	71%

Table 3 lists the parameters that shape the characterization of the clock errors.

The aim of the BWO algorithm is to obtain the combined reduction of both errors in order to achieve the highest levels of accuracy for the TOA and TDOA architectures. Table 4 shows the hyperparameters assumed by the BWO metaheuristic method that allows obtaining an optimized architecture in the proposed scenario.

6.3. Comparative among localization architectures for UAVs localization

The scenario described in Section 6.1 entails a challenge for the sensors' location of each architecture analyzed. Since the localization accuracy is significantly influenced by avoiding the NLOS paths caused by the surrounding buildings, the minimum number of sensors to calculate the target location in each architecture is insufficient to attain an acceptable error bound for the navigation of UAVs in the entire coverage area.

Consequently, a previous study has been conducted to determine the minimum number of sensors to obtain acceptable results. This study revealed that the deployment of 6 sensors enabled the definition of a balanced sensor arrangement to meet the localization objectives of this paper.

In addition, we perform node location optimizations for 8-sensor and 10-sensor configurations to validate the results obtained with 6 sensors and analyze the influence of the variation of the number of sensors in each architecture.

Therefore, we present in Table 5 the localization results obtained for the six optimizations conducted in this paper (i.e., TOA, and TDOA localization architectures for 6-sensor, 8-sensor, and 10-sensor configurations) following the BWO optimization procedure described in Section 5.

As can be seen in Table 5, 10-sensor configurations attain a mean reduction of 26.79% and of 12.35% of the achievable accuracy with regard to 6-sensor and 8-sensor arrangements respectively. Therefore, although 6-sensor configurations can cover the entire TLE region analyzed (i.e., the UAV navigation area) with an error bound contained in 6.25 and 10.04 m in the TDOA and TOA architectures respectively, the consideration of four more sensors significantly improves the localization results without considerably increasing the localization system complexity. This is explained by the consideration of a higher number

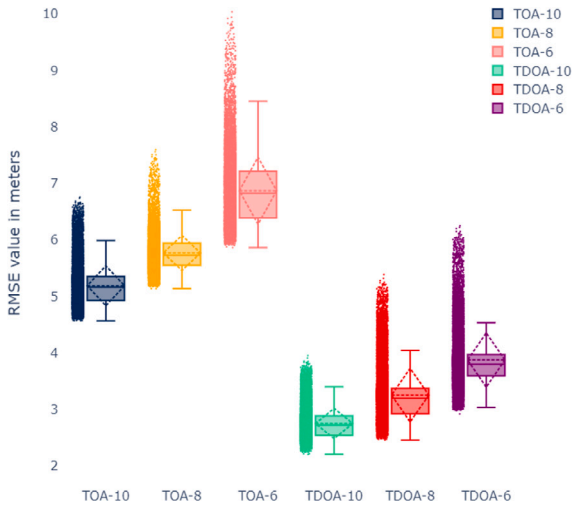

Fig. 3. Comparison of the resulting optimized TOA and TDOA architectures for configurations of 6, 8 and 10 sensors.

Table 5
Localization uncertainty in meters for the TOA and TDOA architectures in the analysis scenario.

Sensors	TDOA			TOA		
	6	8	10	6	8	10
Min	2.92	2.46	2.21	5.86	5.14	4.57
Mean	3.88	3.26	2.75	6.87	5.77	5.19
Median	3.80	3.21	2.72	6.82	5.73	5.17
Max	6.25	5.39	3.95	10.04	7.60	6.76

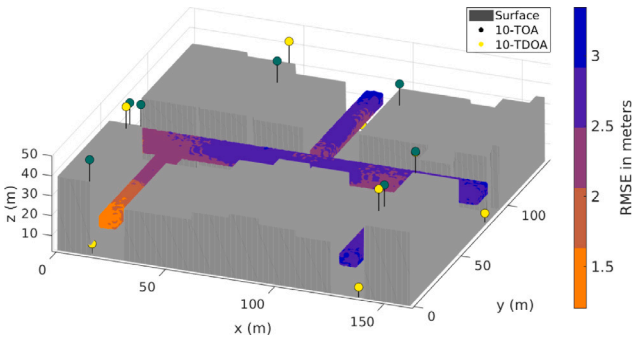

Fig. 4. Reduction of the RMSE obtained by the TDOA architecture with respect to the TOA architecture in 10-sensor configurations. The node location of the TDOA sensors is depicted in yellow while the TOA sensors are represented in green.

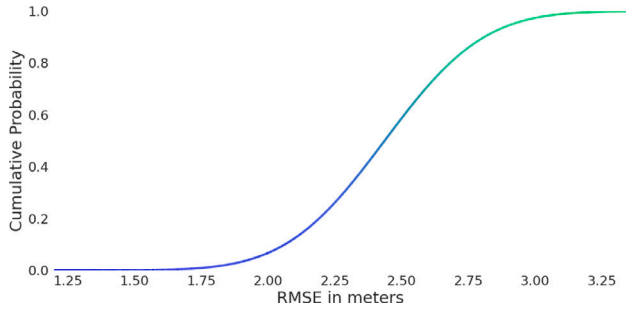

Fig. 5. Cumulative Distribution Function depicting the difference in errors between the TDOA and TOA for the optimized arrangements of 10-sensors.

of time measurements that can be optimally combined to reduce the error bounds as introduced in [26].

The difference among the results obtained of each configuration analyzed is also depicted in Fig. 3.

Fig. 3 shows that not only a reduction of the localization error is achieved through the TDOA architecture as shown in Table 5, but also a lower error variance is reached. Thus, TDOA localization provides a more robust and stable localization system for the navigation of UAVs in urban environments.

The superior results of the TDOA architecture are due to the unnecessary synchronization of the TS clock with the architecture sensors clocks in this architecture. Since the TDOA architecture requires the consideration of two signal paths to collect a time measurement and this fact induces a higher noise error than in the TOA architecture, the only reason for the TDOA to attain lower error bounds is the reduction of the clock errors.

TDOA architecture also requires two different measurement processes to produce a TDOA time measurement which also produces higher clock uncertainties than in the TOA architecture during the measurement process.

Nevertheless, since the synchronization of the TS clock is required in the TOA architecture and this supposes the only factor that can increase the localization error of the TDOA architecture, we can conclude that the synchronization among the TS and the architecture sensors is the principal contributor to the global error of the synchronous time-based localization for UAVs navigation.

This result is in order with previous studies for ground navigation [16] and makes the TDOA architecture stand for deep urban localization.

In addition, the performance of the TOA and TDOA architectures has been compared in a common framework where a BWO process has been performed to optimize the architecture sensors' location. We present in Fig. 4 the final location of the architecture sensors deployed for the final 10-sensor arrangement of the TOA and TDOA architectures.

Furthermore, Fig. 4 shows the lower error bound of the TDOA architecture with regard to the TOA architecture in each TLE point analyzed (i.e., the discretized points representative of the potential UAV navigation area) during the BWO performed. As depicted, the TDOA architecture outperforms the TOA architecture in every analyzed point reducing the error bounds between 1.20 m and 3.35 m in the UAVs navigation area covered by the LPSs deployed.

Fig. 5 introduces the Cumulative Distribution Function (CDF), which illustrates the distribution of the errors calculated in Fig. 4. As can be seen, the TDOA architecture mitigates errors between 1.25 and 2.50 m in comparison to TOA in approximately 60% of the analyzed points, while also exhibiting error reduction between 2.50 and 3.25 m for the remaining localizations.

These results are in order with the principles of each architecture that we introduced in Section 3 and demonstrate the coherence of the results obtained in the BWO performed for each architecture. Furthermore, the optimized sensor arrangements attained allow a direct and fair comparison of the localization results of each architecture since the architectures' dispositions are near-optimal showing the maximal performance achievable by each architecture in the scenario analyzed. This is also justified for the similar locations of the sensors of the TOA and TDOA architecture which have found optimal positions to reduce the NLOS links of the positioning signal in the entire TLE region analyzed.

For this reason, the relevance of the results obtained in our analysis clearly determines the definition of the TDOA architecture for the achievement of more robust, accurate, and stable localization results in synchronous time-based localization methodologies deployed in urban environments.

Finally, we present in Fig. 6 the error distribution in the entire TLE analyzed for the proposed synchronous TDOA architecture with the optimized 10-sensor configuration proposed in this paper for UAVs navigation in urban environments.

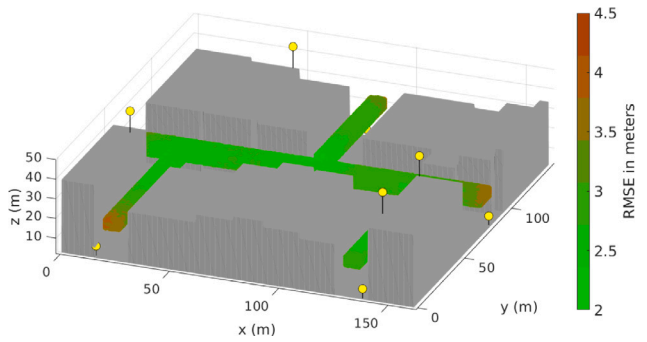

Fig. 6. RMSE result for each TLE point obtained by the optimized 10-sensor TDOA architecture.

The findings depicted in Fig. 6 enhance the results obtained by recent research in UAV localization, which demonstrate an average error of 5 m attributed to various factors, including technology, the utilized algorithm, and suboptimal node placement [35,69].

Hence, our analysis underscores the critical role of these results in shaping the definition of the TDOA architecture for achieving more robust, accurate, and stable localization in synchronous time-based methodologies deployed in urban environments. These insights, as demonstrated in Fig. 6, represent a significant advancement in the field of UAV localization research.

7. Conclusions

UAVs applications are growing over the last few years due to their capacity of automating complex tasks without human intervention. Their applications represent a wide variety of fields such as surveillance, structural inspection, or delivery.

However, the capacity of the UAVs to address complex precision tasks is dependent of the accuracy achieved by their navigation and localization subsystems. This is a remarkable challenge in urban environments, where GNSS localization signals are considerably degraded by NLOS links or multipath effects.

Therefore, we present in this paper, for the first time to the authors' knowledge, the proposal of a comparison between time-based localization architectures to attain competitive localization results for UAV navigation in these challenging environments.

The comparison is made after a black widow optimization procedure to optimally locate the sensor nodes of the two architectures, determining the error bounds of each architecture through a Cramér–Rao Bound characterization considering noise and clock errors.

This allows the determination of the maximal performance of each architecture in the application scenario, which represents a deep urban environment. The results obtained prove the preeminence of the TDOA architecture, thus conforming a more robust, accurate and stable localization system, which contributes to the pursued implementation of UAVs in urban environments.

This relevant conclusion can enhance future research works on this topic by comparing the TDOA architecture with asynchronous positioning methodologies, by improving the results obtained by addressing the discontinuities in the fitness calculations in the boundaries of the scenarios analyzed, or by characterizing other positioning error sources such as multipath.

Declaration of competing interest

The authors declare the following financial interests/personal relationships which may be considered as potential competing interests: Hilde Perez reports financial support was provided by Spanish Ministry of Science and Innovation.

Data availability

Data will be made available on request.

Acknowledgments

This work has been funded by the project of the Spanish Ministry of Science and Innovation grant number PID2019-108277GB-C21/AEI/10.13039/501100011033.

References

[1] S.G. Gupta, D. Ghonge, P.M. Jawandhiya, et al., Review of unmanned aircraft system (UAS), Int. J. Adv. Res. Comput. Eng. Technol. (IJARCET) Vol. 2 (2013).
[2] E. Semsch, M. Jakob, D. Pavlicek, M. Pechoucek, Autonomous UAV surveillance in complex urban environments, in: 2009 IEEE/WIC/ACM International Joint Conference on Web Intelligence and Intelligent Agent Technology, Vol. 2, IEEE, 2009, pp. 82–85.
[3] J. Nikolic, M. Burri, J. Rehder, S. Leutenegger, C. Huerzeler, R. Siegwart, A UAV system for inspection of industrial facilities, in: 2013 IEEE Aerospace Conference, IEEE, 2013, pp. 1–8.
[4] W.-C. Chiang, Y. Li, J. Shang, T.L. Urban, Impact of drone delivery on sustainability and cost: Realizing the uav potential through vehicle routing optimization, Appl. Energy 242 (2019) 1164–1175.
[5] T.M. Fernández-Caramés, O. Blanco-Novoa, I. Froiz-Míguez, P. Fraga-Lamas, Towards an autonomous industry 4.0 warehouse: A UAV and blockchain-based system for inventory and traceability applications in big data-driven supply chain management, Sensors 19 (10) (2019) 2394.
[6] J. Kim, S. Kim, C. Ju, H.I. Son, Unmanned aerial vehicles in agriculture: A review of perspective of platform, control, and applications, IEEE Access 7 (2019) 105100–105115.
[7] T. Pavlenko, M. Schütz, M. Vossiek, T. Walter, S. Montenegro, Wireless local positioning system for controlled UAV landing in GNSS-denied environment, in: 2019 IEEE 5th International Workshop on Metrology for AeroSpace (MetroAeroSpace), IEEE, 2019, pp. 171–175.
[8] S. Bijjahalli, A. Gardi, R. Sabatini, GNSS performance modelling for positioning and navigation in urban environments, in: 2018 5th IEEE International Workshop on Metrology for AeroSpace (MetroAeroSpace), IEEE, 2018, pp. 521–526.
[9] G. Brunner, B. Szebedy, S. Tanner, R. Wattenhofer, The urban last mile problem: Autonomous drone delivery to your balcony, in: 2019 International Conference on Unmanned Aircraft Systems (Icuas), IEEE, 2019, pp. 1005–1012.
[10] M. Arifin, Y. Nazaruddin, T. Tamba, R. Santosa, A. Widyotriatmo, Experimental modeling of a quadrotor uav using an indoor local positioning system, in: 2018 5th International Conference on Electric Vehicular Technology (ICEVT), IEEE, 2018, pp. 25–30.
[11] J. Tiemann, C. Wietfeld, Scalable and precise multi-UAV indoor navigation using TDOA-based uwb localization, in: 2017 International Conference on Indoor Positioning and Indoor Navigation (IPIN), IEEE, 2017, pp. 1–7.
[12] A. Amar, A.J. Weiss, Localization of narrowband radio emitters based on Doppler frequency shifts, IEEE Trans. Signal Process. 56 (11) (2008) 5500–5508.
[13] Y. Wang, X. Ma, G. Leus, Robust time-based localization for asynchronous networks, IEEE Trans. Signal Process. 59 (9) (2011) 4397–4410.
[14] Z. Deng, S. Tang, X. Deng, L. Yin, J. Liu, A novel location source optimization algorithm for low anchor node density wireless sensor networks, Sensors 21 (5) (2021) 1890.
[15] W. Zhao, J. Panerati, A.P. Schoellig, Learning-based bias correction for time difference of arrival ultra-wideband localization of resource-constrained mobile robots, IEEE Robot. Autom. Lett. 6 (2) (2021) 3639–3646.
[16] R. Álvarez, J. Díez-González, P. Verde, H. Perez, Comparative performance analysis of time local positioning architectures in NLOS urban scenarios, IEEE Access 8 (2020) 225258–225271.
[17] N.-T. Nguyen, B.-H. Liu, The mobile sensor deployment problem and the target coverage problem in mobile wireless sensor networks are NP-hard, IEEE Syst. J. 13 (2) (2018) 1312–1315.
[18] J. Díez-González, R. Álvarez, D. González-Bárcena, L. Sánchez-González, M. Castejón-Limas, H. Perez, Genetic algorithm approach to the 3D node localization in TDOA systems, Sensors 19 (18) (2019) 3880.
[19] A. Céspedes-Mota, G. Castañón, A.F. Martínez-Herrera, L.E. Cárdenas-Barrón, Optimization of the distribution and localization of wireless sensor networks based on differential evolution approach, Math. Probl. Eng. 2016 (2016).
[20] J. Díez-González, P. Verde, R. Ferrero-Guillén, R. Álvarez, H. Pérez, Hybrid memetic algorithm for the node location problem in local positioning systems, Sensors 20 (19) (2020) 5475.
[21] N. Vankayalapati, S. Kay, Q. Ding, TDOA based direct positioning maximum likelihood estimator and the cramer-rao bound, IEEE Trans. Aerosp. Electron. Syst. 50 (3) (2014) 1616–1635.

[22] P. Verde, R. Ferrero-Guillén, J.-M. Alija-Pérez, A. Martínez-Gutiérrez, J. Díez-González, H. Perez, Node location optimization for localizing UAVs in urban scenarios, in: International Workshop on Soft Computing Models in Industrial and Environmental Applications, Springer, 2023, pp. 616–625.

[23] P. Verde, J. Díez-González, A. Martínez-Gutiérrez, R. Ferrero-Guillén, R. Álvarez, H. Perez, Black widow optimization for the node location problem in localization wireless sensor networks, in: International Conference on Hybrid Artificial Intelligence Systems, Springer, 2022, pp. 469–480.

[24] J. Díez-González, R. Álvarez, P. Verde, R. Ferrero-Guillén, A. Martínez-Gutiérrez, H. Perez, Optimal node distribution in wireless sensor networks considering sensor selection, in: 16th International Conference on Soft Computing Models in Industrial and Environmental Applications (SOCO 2021), Springer, 2022, pp. 512–522.

[25] D. Bajovic, B. Sinopoli, J. Xavier, Sensor selection for event detection in wireless sensor networks, IEEE Trans. Signal Process. 59 (10) (2011) 4938–4953.

[26] R. Álvarez, J. Díez-Gonzalez, P. Verde, R. Ferrero-Guillén, H. Perez, Combined sensor selection and node location optimization for reducing the localization uncertainties in wireless sensor networks, Ad Hoc Netw. (2023) 103036.

[27] C. Xu, X. Liao, J. Tan, H. Ye, H. Lu, Recent research progress of unmanned aerial vehicle regulation policies and technologies in urban low altitude, IEEE Access 8 (2020) 74175–74194.

[28] M. Elsayed, M. Mohamed, The impact of airspace regulations on unmanned aerial vehicles in last-mile operation, Transp. Res. D 87 (2020) 102480.

[29] M. Garcia, I. Maza, A. Ollero, D. Gutierrez, I. Aguirre, A. Viguria, Release of sterile mosquitoes with drones in urban and rural environments under the European drone regulation, Appl. Sci. 12 (3) (2022) 1250.

[30] M. Mozaffari, W. Saad, M. Bennis, Y.-H. Nam, M. Debbah, A tutorial on UAVs for wireless networks: Applications, challenges, and open problems, IEEE Commun. Surv. Tutor. 21 (3) (2019) 2334–2360.

[31] S. Shakoor, Z. Kaleem, D.-T. Do, O.A. Dobre, A. Jamalipour, Joint optimization of UAV 3-D placement and path-loss factor for energy-efficient maximal coverage, IEEE Internet Things J. 8 (12) (2020) 9776–9786.

[32] M. Samir, S. Sharafeddine, C.M. Assi, T.M. Nguyen, A. Ghrayeb, UAV trajectory planning for data collection from time-constrained IoT devices, IEEE Trans. Wireless Commun. 19 (1) (2019) 34–46.

[33] J. Tan, H. Zhao, UAV localization with multipath fingerprints and machine learning in urban NLOS scenario, in: 2020 IEEE 6th International Conference on Computer and Communications (ICCC), IEEE, 2020, pp. 1494–1499.

[34] A. Couturier, M.A. Akhloufi, A review on absolute visual localization for UAV, Robot. Auton. Syst. 135 (2021) 103666.

[35] T. Liu, H. Zhao, H. Yang, K. Zheng, P. Chatzimisios, Design and implementation of a novel real-time unmanned aerial vehicle localization scheme based on received signal strength, Trans. Emerg. Telecommun. Technol. 32 (11) (2021) e4350.

[36] G. Afifi, Y. Gadallah, Autonomous 3-D UAV localization using cellular networks: deep supervised learning versus reinforcement learning approaches, IEEE Access 9 (2021) 155234–155248.

[37] S. Xu, K. Doğançay, Optimal sensor deployment for 3D AOA target localization, in: 2015 IEEE International Conference on Acoustics, Speech and Signal Processing (ICASSP), IEEE, 2015, pp. 2544–2548.

[38] A. Ledergerber, M. Hamer, R. D'Andrea, A robot self-localization system using one-way ultra-wideband communication, in: 2015 IEEE/RSJ International Conference on Intelligent Robots and Systems (IROS), IEEE, 2015, pp. 3131–3137.

[39] H.-Y. Lin, J.-R. Zhan, GNSS-denied UAV indoor navigation with UWB incorporated visual inertial odometry, Measurement 206 (2023) 112256.

[40] Y. Liu, Y. Wang, Y. Shen, X. Shi, Hybrid TOA-AOA WLS estimator for aircraft network decentralized cooperative localization, IEEE Trans. Veh. Technol. (2023).

[41] R. Ferrero-Guillén, J. Díez-González, P. Verde, R. Álvarez, H. Perez, Table organization optimization in schools for preserving the social distance during the COVID-19 pandemic, Appl. Sci. 10 (23) (2020) 8392.

[42] J. Díez-González, R. Álvarez, L. Sánchez-González, L. Fernández-Robles, H. Pérez, M. Castejón-Limas, 3D tdoa problem solution with four receiving nodes, Sensors 19 (13) (2019) 2892.

[43] R. Álvarez, J. Díez-González, L. Sánchez-González, H. Perez, et al., Combined noise and clock CRLB error model for the optimization of node location in time positioning systems, IEEE Access 8 (2020) 31910–31919.

[44] P. Verde, J. Díez-González, R. Álvarez, H. Perez, Characterization of AGV localization system in industrial scenarios using UWB technology, IEEE Trans. Instrum. Meas. 72 (2023) 1–13.

[45] J. Díez-Gonzalez, R. Álvarez, H. Perez, Optimized cost-effective node deployments in asynchronous time local positioning systems, IEEE Access 8 (2020) 154671–154682.

[46] J. Zhou, L. Shen, Z. Sun, A new method of D-TDOA time measurement based on RTT, in: MATEC Web of Conferences, Vol. 207, EDP Sciences, 2018, p. 03018.

[47] Y.-T. Chan, H.Y.C. Hang, P.-c. Ching, Exact and approximate maximum likelihood localization algorithms, IEEE Trans. Veh. Technol. 55 (1) (2006) 10–16.

[48] L.L. Scharf, L.T. McWhorter, Geometry of the cramer-rao bound, Signal Process. 31 (3) (1993) 301–311.

[49] L. Xiao, L.J. Greenstein, N.B. Mandayam, Sensor-assisted localization in cellular systems, IEEE Trans. Wireless Commun. 6 (12) (2007) 4244–4248.

[50] R. Kaune, J. Hörst, W. Koch, Accuracy analysis for TDOA localization in sensor networks, in: 14th International Conference on Information Fusion, IEEE, 2011, pp. 1–8.

[51] M. Villa, B. Ferreira, N. Cruz, Genetic algorithm to solve optimal sensor placement for underwater vehicle localization with range dependent noises, Sensors 22 (19) (2022) 7205.

[52] S. Yu, J. Zhu, C. Lv, A quantum annealing bat algorithm for node localization in wireless sensor networks, Sensors (ISSN: 1424-8220) 23 (2) (2023) 782.

[53] Y. Xu, O. Ding, R. Qu, K. Li, Hybrid multi-objective evolutionary algorithms based on decomposition for wireless sensor network coverage optimization, Appl. Soft Comput. 68 (2018) 268–282.

[54] F. Domingo-Perez, J.L. Lazaro-Galilea, I. Bravo, A. Gardel, D. Rodriguez, Optimization of the coverage and accuracy of an indoor positioning system with a variable number of sensors, Sensors 16 (6) (2016) 934.

[55] J. Díez-González, R. Álvarez, P. Verde, R. Ferrero-Guillén, H. Perez, Analysis of reliable deployment of TDOA local positioning architectures, Neurocomputing 484 (2022) 149–160.

[56] B. Huang, L. Xie, Z. Yang, TDOA-based source localization with distance-dependent noises, IEEE Trans. Wireless Commun. 14 (1) (2014) 468–480.

[57] R. Álvarez, J. Díez-González, E. Alonso, L. Fernández-Robles, M. Castejón-Limas, H. Perez, Accuracy analysis in sensor networks for asynchronous positioning methods, Sensors 19 (13) (2019) 3024.

[58] R. Alvarez, J. Diez-Gonzalez, N. Strisciuglio, H. Perez, Multi-objective optimization for asynchronous positioning systems based on a complete characterization of ranging errors in 3D complex environments, IEEE Access 8 (2020) 43046–43056.

[59] I. Guvenc, C.-C. Chong, A survey on TOA based wireless localization and NLOS mitigation techniques, IEEE Commun. Surv. Tutor. 11 (3) (2009) 107–124.

[60] Z. Sahinoglu, S. Gezici, I. Guvenc, Ultra-wideband positioning systems, Cambridge, New York, 2008.

[61] J. Karedal, N. Czink, A. Paier, F. Tufvesson, A.F. Molisch, Path loss modeling for vehicle-to-vehicle communications, IEEE Trans. Veh. Technol. 60 (1) (2010) 323–328.

[62] J. Díez-González, R. Alvarez, N. Prieto-Fernández, H. Perez, Local wireless sensor networks positioning reliability under sensor failure, Sensors 20 (5) (2020) 1426.

[63] V. Hayyolalam, A.A.P. Kazem, Black widow optimization algorithm: a novel meta-heuristic approach for solving engineering optimization problems, Eng. Appl. Artif. Intell. 87 (2020) 103249.

[64] P. Verde, J. Díez-González, R. Ferrero-Guillén, A. Martínez-Gutiérrez, H. Perez, Memetic chains for improving the local wireless sensor networks localization in urban scenarios, Sensors 21 (7) (2021) 2458.

[65] D.E. Goldberg, Genetic Algorithms, Pearson Education India, 2013.

[66] L. Cui, C. Xu, G. Li, Z. Ming, Y. Feng, N. Lu, A high accurate localization algorithm with DV-hop and differential evolution for wireless sensor network, Appl. Soft Comput. 68 (2018) 39–52.

[67] T.S. Rappaport, et al., Wireless Communications: Principles and Practice, Vol. 2, prentice hall PTR New Jersey, 1996.

[68] R. Ferrero-Guillén, J. Díez-González, R. Álvarez, H. Pérez, Analysis of the genetic algorithm operators for the node location problem in local positioning systems, in: International Conference on Hybrid Artificial Intelligence Systems, Springer, 2020, pp. 273–283.

[69] R.A. Khalil, N. Saeed, M. Almutiry, UAVs-assisted passive source localization using robust TDOA ranging for search and rescue, ICT Express 9 (4) (2023) 677–682.